Journal of Engineering Physics and Thermophysics, Vol. 77, No. 2, 2004

NONLINEAR EFFECTS IN WATER-VAPOR EXTRACTION FROM A GEOTHERMAL RESERVOIR

C. N. Richardson[a] **and G. G. Tsypkin**[b]

UDC 532.546

The flow of a water–vapor mixture with phase transitions in a geothermal reservoir is considered. The equations were solved using a similarity approach. Linearized equations were considered analytically, and the full nonlinear equations were investigated numerically. It was found that for flows with large gradients of temperature and pressure, the water-saturation function can change nonmonotonically and have a minimum value at some distance from the extraction point. It was shown that if the liquid phase contains dissolved salt then the vaporization process can lead to precipitation of the latter in this low-saturation zone. In the plane of the main parameters, the critical diagram, which distinguishes different regimes of salt precipitation, is constructed.

1. It is known that high-temperature geothermal reservoirs can be saturated with water, vapor, or a water–vapor mixture. Fluid extraction from the formation is accompanied by a pressure drop, which can initiate phase transitions in the extended domain. Using the similarity approach, some problems dealing with water–vapor mixture transport in porous permeable reservoirs have been investigated in [1–3]. In [3], the problem of fluid extraction in a geothermal reservoir was investigated for initially motionless water or vapor. It was shown that for temperatures above 508 K, the water-saturation function can have small deviations from nonmonotonic behavior of less than 1% of the initial value. The nonmonotonic behavior was explained by the physical properties of the heat capacity of the vapor phase at high temperatures.

In this work, two-phase flow was considered, where both phases are initially in motion. In the linear approach, the problem of two-phase flow with phase transitions leads to the solution of an effective equation for temperature. The coefficients of this equation depend only on the physical parameters and initial and boundary conditions of the problem. This solution describes the flow well for permeabilities less than $k < 10^{-17}$ m^2 and for small pressure drops [4]. At high permeabilities and a significant pressure drop, at the extraction point the linear solution breaks down, as the calculated water-saturation function has a negative value. In this case, nonlinear effects are significant, as can be shown by the nonmonotonic water-saturation function obtained by numerical solution of the nonlinear problem. The obtained deviations from the nonmonotonic behavior can be significant and can be as large as the absolute value of the saturation function. The domain in which the saturation function is small and the main part of the volume is occupied by vapor arises as a result of the high rate of vaporization. This domain lies at some distance from the extraction point, while between the minimum point and the well the water content increases. If the liquid phase contains dissolved salt, then the vaporization process leads to increasing concentration, culminating in a maximum at the minimum of water saturation. In this case, as the calculation results show, the salt concentration can exceed the value of salt solubility, resulting in the onset of precipitation. The influence of parameters on salt precipitation is illustrated by the critical diagram.

2. The geothermal reservoir is considered as a horizontal porous permeable stratum with a nondeformable skeletal structure, saturated with a heterogeneous water–vapor mixture. Gravity may be considered as negligible. For the description of heat and mass transfer with equilibrium phase transition, the following system of equations is used.

[a]Institute for Multiphase Flow, University of Cambridge, Madingley Rise, Madingley Road, Cambridge, CB3 OEZ, UK; email: chris@bpi.cam.ac.uk; [b]Institute of Problems of Mechanics, Russian Academy of Sciences, 101 Vernadskii Ave., Moscow, 119526, Russia; email: tsypkin@ipmnet.ru. Translated from Inzhenerno-Fizicheskii Zhurnal, Vol. 77, No. 2, pp. 24–30, March–April, 2004. Original article submitted August 22, 2003.

1062-0125/04/7702-0275 ©2004 Plenum Publishing Corporation

This system is based on conservation laws, Darcy's law [5], the equation of state for water and vapor, the Clausius–Clapeyron equation for water–vapor mixture [6], and thermodynamic relations

$$\phi \frac{\partial}{\partial t} S\rho_{\text{liq}} + \operatorname{div} \rho_{\text{liq}}\mathbf{v}_{\text{liq}} = M\,, \quad \phi \frac{\partial}{\partial t} (1-S)\,\rho_{\text{v}} + \operatorname{div} \rho_{\text{v}}\mathbf{v}_{\text{v}} = -M\,,$$

$$(\rho C)_{\text{m}} \frac{\partial T}{\partial t} + \operatorname{div} (\rho_{\text{liq}} h_{\text{liq}}\mathbf{v}_{\text{liq}} + \rho_{\text{v}} h_{\text{v}}\mathbf{v}_{\text{v}}) = \operatorname{div} (\lambda_{\text{m}} \operatorname{grad} T)\,,$$

$$v_j = -\frac{k}{\mu_j} f_j (S) \operatorname{grad} P\,, \quad j = \text{liq, v}\,, \quad \ln \frac{P}{P_{\text{a}}} = A + \frac{B}{T}\,,$$

$$P = \rho_{\text{v}} RT\,, \quad dh_{\text{liq}} = C_{\text{liq}} dT + \frac{dP}{\rho_{\text{liq}}}\,, \quad dh_{\text{v}} = C_p dT\,, \quad dh_{\text{s}} = C_{\text{s}} dT\,,$$

$$\lambda_{\text{m}} = \phi S\lambda_{\text{liq}} + \phi\,(1-S)\,\lambda_{\text{v}} + (1-\phi)\,\lambda_{\text{s}}\,,$$

$$(\rho C)_{\text{m}} = \phi S\rho_{\text{liq}} C_{\text{liq}} + \phi\,(1-S)\,\rho_{\text{v}} C_p + (1-\phi)\,\rho_{\text{s}} C_{\text{s}}\,.$$

Note that the motion of the mixture is controlled by the compressibility of the vapor phase. Therefore, the density of water may be considered as constant. During extraction of fluid from the geothermal stratum, the pressure in the extracting well drops ($P_{\text{w}} < P_0$), leading to mixture flux for far-field and accompanying vaporization. The vaporization process causes a decrease in temperature towards the well-bore. As initially the mixture was at thermodynamic equilibrium, it is natural to characterize the reservoir by the far-field water-saturation function S_0 and the far-field pressure P_0 or temperature T_0, since they are related by the Clausius–Clapeyron equation.

3. After substitution, the system of basic equations leads to a system of three equations for temperature T, pressure P, and saturation S. We consider the problem in the linear approximation, when changes in the unknown functions are small with respect to their absolute values. Each function is rewritten as the sum of the unperturbed values corresponding to its initial state and small perturbations:

$$S = S_0\,(1 + S')\,, \quad P = P_0\,(1 + P')\,, \quad T = T_0\,(1 + T')\,.$$

After substitution, neglecting higher-order terms, we obtain the following system of equations:

$$S_0 \left(1 - \frac{\rho_{\text{v0}}}{\rho_{\text{liq}}}\right) \frac{\partial S'}{\partial t} + (1-S_0) \frac{\rho_{\text{v0}}}{\rho_{\text{liq}}} \frac{\partial P'}{\partial t} - (1-S_0) \frac{\rho_{\text{v0}}}{\rho_{\text{liq}}} \frac{\partial T'}{\partial t} = \frac{kP_0}{\varphi\mu_{\text{liq}}} \left(f_{\text{liq}}\,(S_0) + f_{\text{v}}\,(S_0) \frac{\mu_{\text{liq}}}{\mu_{\text{v}}} \frac{\rho_{\text{v0}}}{\rho_{\text{liq}}}\right) \Delta P'\,, \tag{1}$$

$$(\rho C)_{\text{m}} T_0 \frac{\partial T'}{\partial t} - \phi S_0 q \rho_{\text{liq}} \frac{\partial S'}{\partial t} + \phi\,(S_0 - 1)\,P_0 \frac{\partial P'}{\partial t} = \lambda_{\text{m}} T_0 \Delta T'\,, \tag{2}$$

$$\frac{P'}{P_0} = F_0 \frac{T'}{T_0}\,, \quad F_0 = -\frac{B}{T_0}\,, \tag{3}$$

$$(\rho C)_{\text{m}} = \phi S_0 \rho_{\text{liq}} C_{\text{liq}} + \phi\,(1-S_0)\,\rho_{\text{v0}} C_p + (1-\phi)\,\rho_{\text{s}} C_{\text{s}}\,,$$

$$\lambda_{\text{m}} = \phi S_0 \lambda_{\text{liq}} + \phi\,(1-S_0)\,\lambda_{\text{v}} + (1-\phi)\,\lambda_{\text{s}}\,, \quad q = h_{\text{v}} - h_{\text{liq}}\,.$$

In Eqs. (1), (2), the perturbation of the water-saturation function only appears as a time derivative. These derivatives can be eliminated from the system, while the pressure perturbations can be eliminated using Eq. (3). As a result, we have an effective diffusion equation with coefficients dependent on the physical parameters of the system and initial conditions:

$$(\rho C)_{\text{eff}} \frac{\partial T'}{\partial t} = \lambda_{\text{eff}} \Delta T', \quad (\rho C)_{\text{eff}} = R_1 + R_2, \tag{4}$$

$$\lambda_{\text{eff}} = R_3 \frac{q\rho_{\text{v0}}}{\varepsilon} + R_4, \quad \varepsilon = \frac{\rho_{\text{v0}}}{\rho_{\text{liq0}}}, \quad R_4 = \frac{kq}{\phi\mu_{\text{v}}} (1 - S_0) P_0 F_0 \rho_{\text{v0}} + \lambda_{\text{m}} \frac{T_0}{\phi},$$

$$R_1 = S_0 + (1 - S_0)(1 - F_0)\varepsilon, \quad R_3 = \frac{kP_0 T_0}{\phi} \left(\frac{S_0}{\mu_{\text{liq}}} + \frac{1 - S_0}{\mu_{\text{v}}} \varepsilon \right),$$

$$R_2 = T_0 \frac{(\rho C)_{\text{m}}}{\phi} + (1 - S_0) q\rho_{\text{v0}} + P_0 F_0 \left(S_0 + \frac{q(1 - S_0)}{RT_0} - 1 \right).$$

For the sake of simplicity, we consider only relative permeability functions:

$$f_{\text{liq}}(S) = S, \quad f_{\text{v}}(S) = 1 - S.$$

Note that as pressure and temperature are related by Eq. (3), an equation analogous to (4) can be found for the pressure distribution. In order to obtain the water-saturation function from the system (1)–(3), the terms with spatial derivatives must be eliminated. As a result, the following equation connecting the time derivative of temperature (or equivalently pressure) and the time derivative of water saturation can be constructed:

$$\left[R_2 - R_4 \frac{R_1}{R_3} \right] \frac{\partial T'}{\partial t} = S_0 \left[\frac{q}{RT_0} + \varepsilon \frac{R_4}{R_3} \right] \frac{\partial S'}{\partial t}. \tag{5}$$

If the initial values of pressure P_0, water saturation S_0, and pressure in the well P_{w} are constant, the one-dimensional problem in a semi-infinite domain admits a similarity solution:

$$T = T(\zeta), \quad P = P(\zeta), \quad S = S(\zeta), \quad \zeta = \frac{x}{\sqrt{t\kappa_{\text{a}}}}, \quad \kappa_{\text{liq}} = \frac{kP_0}{\phi\mu_{\text{liq}}}, \quad \kappa_{\text{a}} = \frac{kP_{\text{a}}}{\phi\mu_{\text{liq}}}.$$

The value of the functions at $x = 0$ corresponds to their values at the boundary between the stratum and the well. In this case, the distributions of temperature and pressure can be found from Eq. (4) and those of the water saturation from Eq. (5):

$$T(\zeta) = (T_{\text{w}} - T_0) \operatorname{erfc}\left(\frac{\zeta}{2} \sqrt{\frac{\kappa_{\text{a}}}{a_{\text{eff}}}} \right) + T_0, \quad S(\zeta) = \sigma \left(\frac{T(\zeta)}{T_0} - 1 \right) + S_0, \tag{6}$$

where

$$\sigma = \frac{R_2 R_3 - R_1 R_4}{R_5 + (1 - \varepsilon) R_4}; \quad R_5 = \frac{q}{RT_0}; \quad a_{\text{eff}} = \frac{\lambda_{\text{eff}}}{(\rho C)_{\text{eff}}}.$$

If the pressure in the well P_{w} is fixed, then the mixture temperature is defined by Eq. (3) and the saturation by Eq. (6):

$$S_{\mathrm{w}} = \sigma\left(\frac{T_{\mathrm{w}}}{T_0} - 1\right) + S_0 \,. \tag{7}$$

Calculations were made at the following values of physical parameters: $\rho_{\mathrm{s}} = 2.5\cdot10^3$ kg/m^3, $\rho_{\mathrm{liq}} = 0.9\cdot10^3$ kg/m^3, $\lambda_{\mathrm{s}} = 2$ W/(m·K), $\lambda_{\mathrm{liq}} = 0.58$ W/(m·K), $C_{\mathrm{s}} = 10^3$ J/(kg·K), $C_{\mathrm{liq}} = 4.2\cdot10^3$ J/(kg·K), $R = 461$ J/(kg·K), $q = 2.26\cdot10^6$ J/kg, $\mu_{\mathrm{liq}} = 2\cdot10^{-4}$ Pa·sec, $\mu_{\mathrm{v}} = 1.3\cdot10^{-5}$ Pa·sec, $P_{\mathrm{a}} = 10^5$ Pa, and $\phi = 0.2$.

Simple calculations show that if pressure decreases in the well, the water saturation in the well also decreases and can have a negative value, although this is physically impossible. If the value of the permeability is large enough, a small deviation from the initial pressure (when $P - P_{\mathrm{w}} \ll P_0$) leads to a negative value of the saturation function. For example, if $T_0 = 450$ K ($P_0 = 9.619\cdot10^5$ Pa), $S_0 = 0.5$, $P_{\mathrm{w}} = 8\cdot10^5$ Pa, and $k = 10^{-17}$ m^2, then the saturation function at the well $S_{\mathrm{w}} = 0.47$; when $k = 10^{-16}$ m^2, $S_{\mathrm{w}} = 0.298$; and when $k = 10^{-14}$ m^2, $S_{\mathrm{w}} = -0.0468$. It is natural to assume that the reason for this behavior is the significant nonlinearity of the water–vapor mixture flow, as the perturbation of the saturation function is comparable to its value. In the following section, the nonlinear problem will be investigated and a comparison made with the results above.

4. In the self-similar formulation, the dimensionless nonlinear system of the main equations for pressure, temperature, and water saturation has the form

$$\frac{dS}{d\zeta}\left[\frac{\zeta}{2}\left(1 - \varepsilon\frac{\hat{P}}{\hat{T}}\right) + \frac{d\hat{P}}{d\zeta}\left(\delta_{\mathrm{liq}} f'_{\mathrm{liq}} + \varepsilon\delta_{\mathrm{v}} f'_{\mathrm{v}}\frac{\hat{P}}{\hat{T}}\right)\right] + \frac{d^2\hat{P}}{d\zeta^2}\left[\delta_{\mathrm{liq}} f_{\mathrm{liq}} + \varepsilon\delta_{\mathrm{v}} f_{\mathrm{v}}\frac{\hat{P}}{\hat{T}}\right] =$$

$$= -\left[\frac{1}{\hat{P}} - \frac{1}{\hat{T}}\frac{d\hat{T}}{d\hat{P}}\right]\varepsilon\frac{\hat{P}}{\hat{T}}\frac{d\hat{P}}{d\zeta}\left[\delta_{\mathrm{v}} f_{\mathrm{v}}\frac{d\hat{P}}{d\zeta} + (1-S)\frac{\zeta}{2}\right],$$

$$\frac{dS}{d\zeta}\left[\frac{\zeta}{2} - \Lambda\frac{d\hat{P}}{d\zeta}\frac{d\hat{T}}{d\hat{P}} + \delta_{\mathrm{liq}} f'_{\mathrm{liq}}\frac{d\hat{P}}{d\zeta}\right] + \frac{d^2\hat{P}}{d\zeta^2}\left[\delta_{\mathrm{liq}} f_{\mathrm{liq}} - \Lambda\,(\Lambda_{\mathrm{s,liq}} + S)\frac{d\hat{T}}{d\hat{P}}\right] =$$

$$= -(1-S)\frac{P_0}{q\rho_{\mathrm{liq}}}\frac{\zeta}{2}\frac{d\hat{P}}{d\zeta} + C\frac{\zeta}{2}\frac{d\hat{P}}{d\zeta}\frac{d\hat{T}}{d\hat{P}}(C_{\mathrm{s,liq}} + S) + C\delta_{\mathrm{liq}} f_{\mathrm{liq}}\frac{d\hat{T}}{d\hat{P}}\left(\frac{d\hat{P}}{d\zeta}\right)^2 + \tag{8}$$

$$+ \delta_{\mathrm{liq}}\frac{P_0}{q\rho_{\mathrm{liq}}} f_{\mathrm{liq}}\left(\frac{d\hat{P}}{d\zeta}\right)^2 + \Lambda\,(\Lambda_{\mathrm{s,liq}} + S) + \frac{d^2\hat{T}}{d\hat{P}^2}\left(\frac{d\hat{P}}{d\zeta}\right)^2,$$

$$\ln\frac{P_0}{P_{\mathrm{a}}}\hat{P} = A + \frac{B}{T_0}\frac{1}{\hat{T}};$$

here

$$\hat{P} = \frac{P}{P_0};\quad \hat{T} = \frac{T}{T_0};\quad \kappa_{\mathrm{v}} = \frac{kP_0}{\phi\mu_{\mathrm{v}}};\quad \Lambda = \frac{\lambda_{\mathrm{liq}} T_0}{q\rho_{\mathrm{liq}}\kappa_{\mathrm{a}}};\quad \Lambda_{\mathrm{s,liq}} = \frac{\lambda_{\mathrm{s}}(1-\phi)}{\lambda_{\mathrm{liq}}\phi};\quad C = \frac{C_{\mathrm{liq}} T_0}{q};$$

$$C_{\mathrm{s,liq}} = \frac{\rho_{\mathrm{s}} C_{\mathrm{s}}(1-\phi)}{\rho_{\mathrm{liq}} C_{\mathrm{liq}}\phi};\quad \delta_{\mathrm{liq}} = \frac{\kappa_{\mathrm{liq}}}{\kappa_{\mathrm{a}}};\quad \delta_{\mathrm{v}} = \frac{\kappa_{\mathrm{v}}}{\kappa_{\mathrm{a}}}.$$

The system of equations (8) was solved numerically for the same values of parameters as in the previous section. Figure 1 illustrates the close agreement between the linear and nonlinear solutions for the saturation function in the case of low values of permeability, when the pressure in the well has the same order as the initial pressure. However, even in this case there is a noticeable difference in the saturation function in the domain near the well. If the pressure in the well drops significantly, the behavior of the water-saturation function can be nonmonotonic. The distributions of

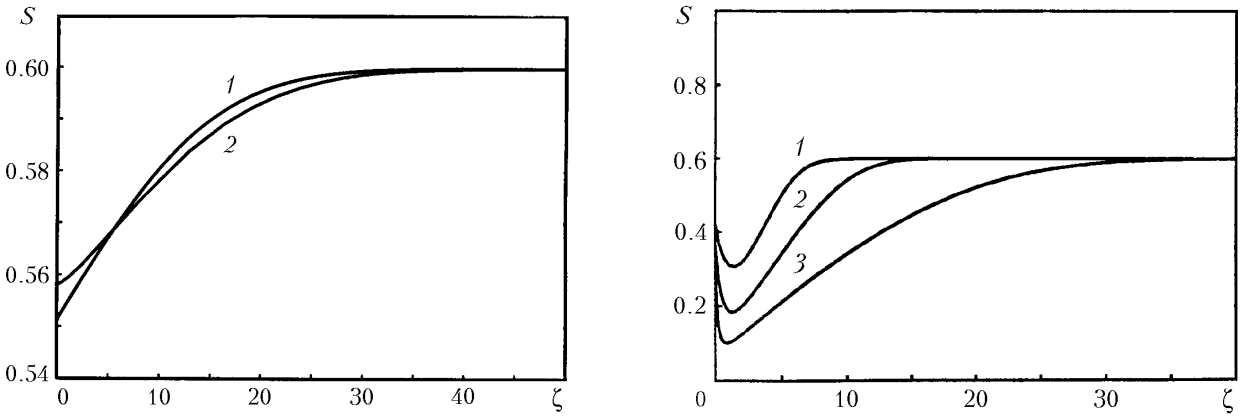

Fig. 1. Distributions of the water-saturation function for linear (1) and nonlinear (2) solutions.

Fig. 2. Nonmonotonic distributions of water-saturation for different initial conditions at $k = 10^{-16}$ m^2, $P_w = 2 \cdot 10^5$ Pa, and $S_0 = 0.6$; 1) $P_0 = 10^6$ Pa; 2) $P_0 = 3 \cdot 10^6$ Pa; 3) $P_0 = 10^7$ Pa.

the pressure and temperature are always monotonic. In Fig. 2, the typical nonmonotonic distributions of the water-saturation function are shown for different formation pressures. Increasing formation pressure intensifies the flow rate and vaporization rate of the mixture. As a result, the phase-transition domain increases and the minimum value of saturation decreases.

In order to analyze the behavior of the water-saturation function, some simplifying assumptions should be made. Let us assume that the saturation at no point takes a value less than one tenth of its initial value, for example, as in Fig. 2. Secondly, the viscosities and densities of vapor and water satisfy the relation

$$\frac{\mu_{liq}\rho_v}{\mu_v\rho_{liq}} << 1 .$$

Lastly, the thermodynamic state should not be near the critical point for water. Then, neglecting small terms in the first equations of (8), we obtain the following simplified equation:

$$\frac{\partial S}{\partial t} - \delta_{liq}\left(\frac{\partial S}{\partial x}\frac{\partial \hat{P}}{\partial x} + S\frac{\partial^2 \hat{P}}{\partial x^2}\right) = 0 .$$

In the similarity approach, the derivative of S is defined by

$$S'_\zeta = \frac{-\delta_{liq} S \hat{P}''_{\zeta\zeta}}{0.5\zeta + \delta_{liq}\hat{P}'_\zeta} .$$

The denominator on the right-hand side of the equation is always positive. Therefore, the sign of the derivative of S is determined by the sign of the second derivative of pressure. The minimum of saturation is reached at the point where the second derivative of pressure is zero.

5. Decrease in the water-saturation function during mixture extraction from the geothermal reservoir is a very important factor when the liquid phase contains dissolved salt. Vaporization of the solution leads to a growth in salt concentration and ultimately salt precipitation, clogging the permeable formation and bringing extraction to a halt. It is assumed that dissolved salt plays only a passive role and does not affect the physical parameters of the solution or the position of the Clausius–Clayperon curve in the (P, T) phase plane. In this case, the system of basic equations of heat and mass transfer must be supplemented by a salt conservation law, which is usually expressed as

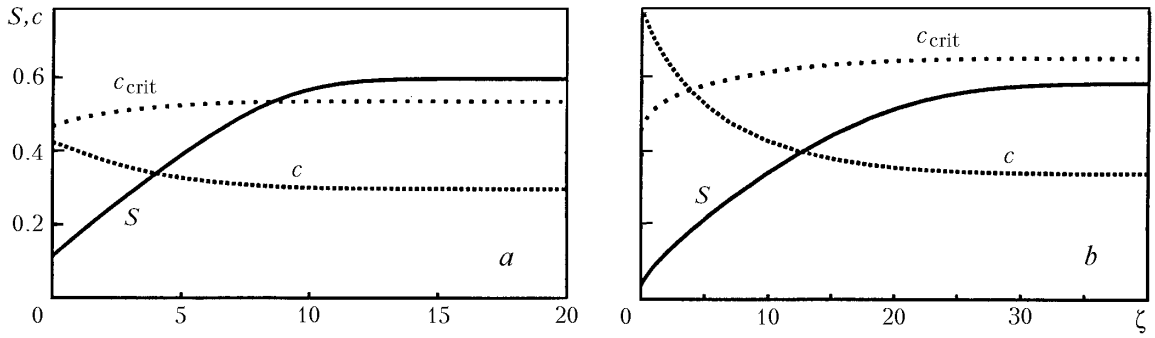

Fig. 3. Distributions of salt concentration and solubility at $k = 10^{-14}$ m^2, $P_w = 10^6$ Pa, and $S_0 = 0.6$; a) $P_0 = 3 \cdot 10^6$ Pa; b) $P_0 = 10^7$ Pa.

$$\phi \frac{\partial}{\partial t} (S\rho_{liq} c) + \text{div} (\rho_{liq} c \mathbf{v}_{liq} - \phi D S \rho_{liq} \text{ grad } c) = 0 . \tag{9}$$

Note that since vaporization due to motion of the mixture occurs as a result of pressure drop, the typical length scale of the phase-transition domain is determined by the parameter $\kappa_v >> D$. Also, since there are no sharp phase-transition fronts, the effects of salt diffusion may be neglected. In the case of self-similar solution of the problem of salt distribution, the concentration of salt can be found from the following equation derived from (9):

$$(\ln c)'_\zeta = \frac{0.5 S'_\zeta + \delta_{liq} S'_\zeta \hat{P}'_\zeta + \delta_{liq} S \hat{P}''_{\zeta\zeta}}{0.5 S + \delta_{liq} S \hat{P}'_\zeta} .$$

If the initial salt concentration is large and the water-saturation function varies considerably, then salt concentration can reach the saturation value, which is a function of temperature and can be determined by approximation of experimental data in the form

$$c_{crit} \left(\frac{T_0}{373.15} \hat{T} \right) = 0.56355 - 0.59237 \left(\frac{T_0}{373.15} \hat{T} \right) + 0.42265 \left(\frac{T_0}{373.15} \hat{T} \right)^2 .$$

The solution of the problem is valid for concentration values not larger than the solubility:

$$c(\zeta) \le c_{crit}(\zeta) = c_{crit} \left(\frac{T_0}{373.15} \hat{T}(\zeta) \right). \tag{10}$$

In Fig. 3a, typical distributions of the water-saturation function, salt concentration, and solubility are shown in the case where the water-saturation function is monotonic. It is seen that the salt concentration does not exceed the solubility value. For large initial pressures the flow rate increases, intensifying the vaporization process and correspondingly the salt-accumulation process. If the rate of vaporization is high enough, the salt concentration can exceed the critical value of solubility, causing the onset of salt precipitation (Fig. 3b). The model cannot be applied to the salt precipitation itself. If all functions are monotonic, salt precipitation can only take place adjacent to the well. In the case of nonmonotonic behavior of the water-saturation function, another regime of salt accumulation exists. In Fig. 4a, the case of nonmonotonic behavior of the water-saturation function is shown. It is evident that the salt distribution will also have a nonmonotonic character, and the domain of maximum salt concentration will correspond to the minimum of saturation. For low vaporization rates, corresponding to small values of the initial pressure, the increase in salt concentration is small and does not exceed the solubility at a local temperature. If the initial pressure is large enough, a high rate of vaporization leads to a correspondingly high rate of increase of salt concentration, which can be larger than the solubility (Fig. 4b). However, in the last case, the maximal value is reached at some distance from the well. This means that the extended domain of salt precipitation will also lie away from the well and the region adjacent to the

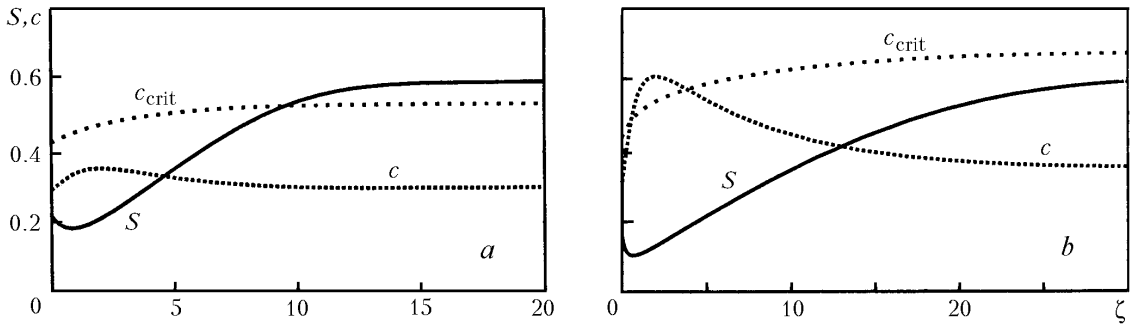

Fig. 4. Nonmonotonic distributions of saturation and salt concentration for $k = 10^{-16}$ m^2, $P_w = 5 \cdot 10^5$ Pa, and $S_0 = 0.6$; a) $P_0 = 3 \cdot 10^6$ Pa; b) $P_0 = 10^7$ Pa.

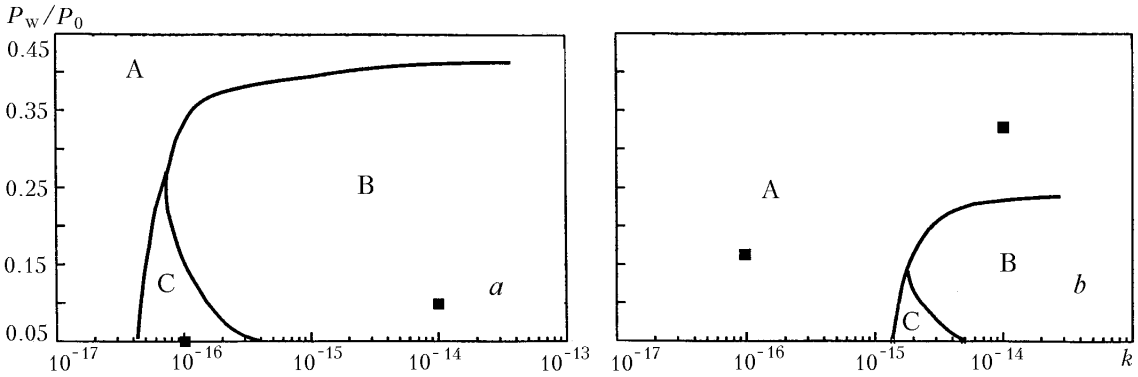

Fig. 5. Critical diagram.

well will be saturated by a water–vapor mixture. In the case of salt precipitation, a part of the porous permeable matrix will be filled with solid salt, leading to a reduction of porosity and permeability. Changes in porosity or permeability cannot be addressed using our model; however, useful information about different regimes of salt precipitation can be obtained.

In Fig. 5, a critical diagram showing the influence of the main parameters on the vaporization process is presented. There are three domains, corresponding to different kinds of solution. If the parameters lie within domain A, then salt precipitation does not take place. This regime corresponds to the extraction regimes with small permeability and pressure gradient. An increase in permeability or decrease in well pressure leads to intensification of the vaporization process and a decrease in volume of the liquid phase and a respective growth of salt concentration. At some value of the parameters, corresponding to the critical curves, the obtained concentrations coincide with the solubility. In domains B and C, the salt concentration exceeds the solubility and salt precipitation sets in. Domain B corresponds to salt precipitation near the extracting well, while domain C is characterized by nonmonotonic behavior of the water-saturation function and salt precipitates at some distance from the well-bore. The critical diagram shows that at high initial pressures and temperatures a high-intensity regime of vaporization takes place (Fig. 5a) and domains B and C are comparatively large. For low-intensity regimes (Fig. 5b), the salt-precipitation domain shrinks and includes only the high-permeability range. The fluid-extraction regime can be regulated by change of the well pressure P_w. Therefore, as the diagram shows, it is possible to reduce the risk of salt precipitation by increasing the well pressure P_w.

6. In the present work, we have investigated the behavior of an equilibrium water–vapor mixture in a geothermal reservoir in the case where the saturation function is nonmonotonic. As a rule, geothermal reservoirs are characterized by a high amount of salt in a dissolved form. As a result of vaporization, there will be a zone of low water saturation in the formation which may initiate salt precipitation in the geothermal reservoir. Salt precipitation leads to clogging and a drop in productivity of the extracting well and can even shut down the well altogether. If clogging occurs directly adjacent to the well, it may be possible to remediate the situation by some means. However, if clogging occurs at some distance from the well it will be much more difficult. It is therefore important to know which regime

is applicable to an operating well in order to avoid at all costs the latter regime. Moreover, by increasing the well pressure it is possible to reach an extraction regime with no salt precipitation in the geothermal reservoir.

This work was supported by the BP Institute for Multiphase Flow (University of Cambridge) and the Russian Foundation for Fundamental Research (grant No. 03-01-00068).

NOTATION

a, thermal diffusivity, m^2/sec; *c*, salt concentration, kg/kg; *C*, specific heat, J/(K·kg); C_p, specific heat at constant pressure, J/(K·kg); *D*, diffusion coefficient, m^2/sec; *h*, specific enthalpy, J/kg; *k*, permeability, m^2; *M*, vaporized mass, kg; *P*, pressure, Pa; *q*, specific heat of vaporization, J/kg; *R*, gas constant, J/(kg·K); *S*, saturation of water; *T*, temperature, K; *t*, time, sec; *v*, filter velocity, m/sec; *x*, coordinate, m; ζ, dimensionless similarity variable; λ, thermal conductivity, W/(m·K); μ, viscosity, Pa·sec; ρ, density, kg/m^3; ϕ, porosity, m^3/m^3. Subscripts: a, atmospheric value; crit, critical value; ef, effective value; f', perturbation of function *f*; 0, initial value; liq, liquid; m, mixture; s, porous medium skeleton; v, vapor; w, value at the well.

REFERENCES

1. M. L. Sorey, M. L. Grant, and E. Bradford, Nonlinear effects in two-phase flow to wells in geothermal reservoirs, *Water Resour. Res.*, **16**, 767–777 (1980).
2. M. J. O'Sullivan, A similarity method for geothermal well test analysis, *Water Resour. Res.*, **17**, 390–398 (1981).
3. J. G. Burnell, A. McNabb, G. J. Weir, and R. Young, Two-phase boundary layer formation in a semi-infinite porous slab, *Transport Porous Media*, **4**, 395–420 (1989).
4. G. G. Tsypkin, On the rise of two mobile boundaries of phase transition under vapor extraction from a geothermal water-saturated stratum, *Dokl. Ross. Akad. Nauk*, **337**, No. 6, 749–751 (1994).
5. M. J. O'Sullivan, Geothermal reservoir simulation, *Int. J. Energy Res.*, **9**, 319–332 (1985).
6. M. P. Vukalovich, *Thermodynamic Properties of Water and Water Vapor* [in Russian], Moscow (1955).